Engineering Journal of Qatar University, Vol. 7, 1994, p. 151 - 170

# CHEBYSHEV EXPANSION OF THE FLOW IN A SPINNING AND CONING CYLINDER

**Mohamed Selmi**
Assistant Professor of Mechanical Engineering
University of Qatar, Doha, Qatar.

## ABSTRACT

This paper is concerned with the calculation of the moments exerted by a viscous fluid on the walls of a cylinder that is spinning about its axis and coning about an axis that passes through its center of mass. For small coning angles and/or coning frequencies, these moments are estimated by solving the linearized Navier-Stokes equations. Solving the linearized Navier-Stokes equations is computationally expensive. Fortunately, when using the control volume approach to calculate these moments, these moments depend essentially on the axial velocity, and the linearized equations describing the deviation of the fluid motion from solid body rotation can be reduced to a single sixth-order partial differential equation governing the axial velocity. This single equation is solved by expanding the axial velocity in a triple series made of Fourier functions in the azimuthal direction and Chebyshev polynomials in the radial and axial directions. For linear analysis, only the fundamental component in the azimuthal direction is needed for the evaluation of moments and the triple series is reduced to a double Chebyshev expansion in the radial and axial directions thereby reducing the three-dimensional problem into a two-dimensional one. The results obtained by Chebyshev expansion show good agreement with those obtained by using eigenfunction expansion.

## INTRODUCTION

Spin-stabilized liquid-filled projectiles are known to experience severe dynamical instabilities owing to the motion of their liquid payload. For cylinders completely filled with a single fluid we know two types of instabilities that are excited by the coning motion of the projectile about its flight trajectory. One of the instabilities is caused by resonance with inertial waves at critical coning frequencies (ratio of the coning rate $\Omega$ to the spin rate $\omega$) and is most pronounced for fluids of low viscosity, i.e. high Reynolds numbers. We define the Reynolds number as $\mathrm{Re}=\omega a^2/\nu$, where $a$

is the radius of the cylinder and $\nu$ is the kinematic viscosity of the liquid. This instability is known to strongly depend on the cylinder aspect ratio (ratio of the length $2c$ of the cylinder to its diameter $2a$). For stable designs, the aspect ratio is properly chosen to avoid resonance for a given coning frequency. The other kind of instabilities is due to viscous stresses applied on the walls of the payload container and is most pronounced for fluids of high viscosity, i.e. low to medium Reynolds numbers, for a wide range of aspect ratios and coning frequencies.

Quite a few theories, employing different approximations, have been proposed for the purpose of understanding both types of instabilities and, to gain capabilities in the evaluation of the moments caused by the liquid payload. The Stewartson-Wedemeyer theory (Stewartson 1959; Wedemeyer 1966) employs the boundary-layer approximation as a basis. Since this approximation is only valid for flows at sufficiently large Reynolds numbers, say $Re \geq 1000$, the theory is primarily suited to predict instability caused by inertial waves. Analysis based on the Navier-Stokes equations (Herbert & Li 1987, 1990) shows, however, that resonance with inertial waves may severely influence the liquid moments at Reynolds numbers as low as $Re = 100$.

An improvement to the Stewartson-Wedemeyer theory has been proposed by Kitchens, Gerber, and Sedney (KGS) (see for example Murphy 1991). While the Stewartson-Wedemeyer theory uses the boundary layer approximation in both the radial and axial directions, the KGS method employs the boundary layer approximation only in the axial direction and solves the linearized Navier-Stokes equations in the radial direction.

A method for solving the full linearized Navier-Stokes equations has been suggested by Hall, Sedney, and Gerber (HSG) (Hall et al. 1990). This approach expands velocity components and pressure in a series of products of complex trigonometric functions in axial direction and radial "eigenfunctions" that satisfy homogeneous boundary conditions at the side wall. The expansion coefficients of the series can be found from the boundary conditions at the end walls by collocation or least squares. While this method has the potential of treating both types of instabilities, its shortcoming is in the numerical determination of eigenvalues and eigenfunctions. For given parameters, the eigenvalues for the HSG expansion are obtained by iterative solution of a sixth-order complex system of ordinary differential equations and are difficult to find. Good initial guesses are

required for the iteration to converge. This problem is currently overcome by precalculating voluminous tables for interpolation from the initial estimates.

Selmi, Li, and Herbert (SLH) (Selmi et al. 1992) have developed an alternative method to calculating the moments from the full linearized Navier-Stokes equations. The SLH approach is based on the observation that when using a control volume analysis to calculate the moments, these moments depend essentially on the axial velocity. They have derived a single sixth-order partial differential equation for the axial velocity component and solved it by eigenfunction expansion. The eigenfunctions are given in closed form and the eigenvalues are determined by numerically solving a system of closed form characteristic equations. Since the eigenfunctions are given in closed form, their analytical integrability leads to accurate evaluation of the moments when using the control volume formulation.

The eigenvalue problem associated with the SLH method is a sixth-order complex eigenvalue problem and is quite difficult to solve. Accounting for all eigenvalues especially near the origin of the complex plane is crucial to the convergence of the method. Here, we present an alternative method to solving the sixth-order partial differential equation governing the axial velocity by Chebyshev expansion and compare the results with those obtained by eigenfunction expansion of Selmi et al. (1992).

## GOVERNING EQUATIONS

We consider the steady flow of a viscous fluid of density $\rho$ and viscosity $\mu$ inside a cylinder of radius $a$ and length $2c$. The cylinder is rotating about its axis at the spin rate $\omega$ and rotating about an axis that passes through its center of mass at the coning rate $\Omega$. We use Cartesian coordinates $x$, $y$, $z$, where $z$ is the spin axis and $x$ is normal to $z$ and coplanar with both the spin axis and the coning axis $Z$. The angle between spin axis and coning axis is denoted by $\theta$, as shown in figure 1. The governing equations of the motion of the fluid inside the cylinder represent both conservation of mass and momentum. When written with respect to the coning system ($x$, $y$, $z$), that rotates about the $Z$-axis of the inertial system ($X$, $Y$, $Z$) at the coning rate $\Omega$, they take the form

$$\nabla \cdot \mathbf{V} = 0, \tag{1a}$$

$$\rho\left[\frac{D\mathbf{V}}{Dt}+2\Omega\hat{\mathbf{k}}\times\mathbf{V}+\Omega\hat{\mathbf{k}}\times\left(\Omega\hat{\mathbf{k}}\times\mathbf{r}\right)\right]=-\nabla P+\mu\nabla^2\mathbf{V}, \qquad (1b)$$

where $\mathbf{V}$ and $P$ denote the velocity and pressure respectively, $\hat{\mathbf{k}}$ is a unit vector in the Z direction, and $\mathbf{r}$ is the position vector.

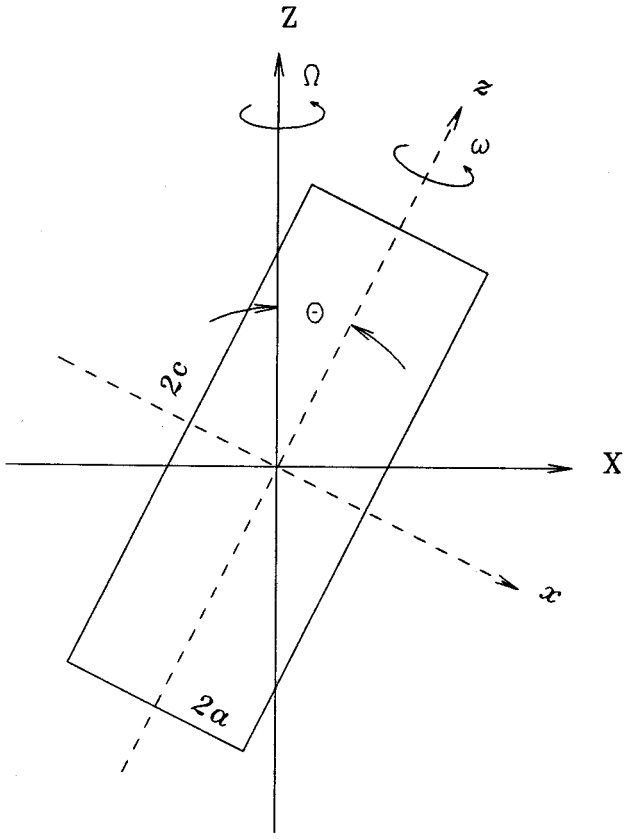


**Figure 1: Description of geometry**

The flow quantities are made dimensionless by using ρ to scale mass, $a$ to scale length, and ω to scale time. The problem then depends on the aspect ratio $\eta=a/c$, the coning frequency $\tau=\Omega/\omega$, the coning angle θ, and the Reynolds number $\mathrm{Re} = \omega a^2/\nu$, where ν denotes the kinematic viscosity. Hence, from here on all flow quantities are dimensionless. They are also best described in cylindrical coordinates $(r, \phi, z)$, where $r$ is in the radial direction, $\phi$ is in the azimuthal direction, and $z$ is in the axial direction.

Moreover, it is convenient to split the velocity and pressure (Herbert 1985) according to

$$\mathbf{V} = \mathbf{v}^s + \mathbf{v}, \tag{2a}$$

$$P = p^s + p^d, \tag{2b}$$

where $\mathbf{v}^s = r\,\mathbf{e}_\phi$ with $\mathbf{e}_\phi$ denoting a unit vector in the azimuthal direction, is the velocity due to solid-body rotation, and $p^s$ is chosen so that the forcing terms in the governing equations reduce to only one term present in the $z$-momentum equation,

$$p^s = \tfrac{1}{2}\left[r^2(1+\tau_z)^2 + r^2\tau_\phi^2 + z^2\varepsilon^2 - 2rz\tau_z\tau_r\right], \tag{3}$$

where $\tau_r = -\varepsilon\cos(\phi)$, $\tau_\phi = \varepsilon\sin(\phi)$, $\tau_z = \tau\cos(\theta)$, and $\varepsilon = \tau\sin(\theta)$.

The equations governing the cylindrical components $v_r$, $v_\phi$, $v_z$ of the deviation of the velocity from solid-body rotation and the perturbation pressure $p^d$ have been derived by Herbert (1985). They take the form

$$\frac{1}{r}\frac{\partial}{\partial r}(rv_r) + \frac{\partial}{\partial\phi}(v_\phi) + \frac{\partial}{\partial z}(v_z) = 0, \tag{4}$$

$$D'v_r - \frac{v_\phi^2}{r} - 2(1+\tau_z)v_\phi + 2\tau_\phi v_z = -\frac{\partial p^d}{\partial r} + \frac{1}{\mathrm{Re}}\left[D''v_r - \frac{v_r}{r^2} - \frac{2}{r^2}\frac{\partial v_\phi}{\partial\phi}\right], \tag{5}$$

$$D'v_\phi - \frac{v_r v_\phi}{r} + 2(1+\tau_z)v_r - 2\tau_r v_z = -\frac{1}{r}\frac{\partial p^d}{\partial\phi} + \frac{1}{\mathrm{Re}}\left[D''v_\phi - \frac{v_\phi}{r^2} + \frac{2}{r^2}\frac{\partial v_r}{\partial\phi}\right], \tag{6}$$

$$D'v_z - \frac{v_\phi^2}{r} + 2\tau_r v_\phi - 2\tau_\phi v_r = -\frac{\partial p^d}{\partial z} - 2r\tau_r + \frac{1}{\mathrm{Re}}\left[D''v_z\right], \tag{7}$$

where

$$D' = \frac{\partial}{\partial t} + \frac{\partial}{\partial\phi} + v_r\frac{\partial}{\partial r} + \frac{v_\phi}{r}\frac{\partial}{\partial\phi} + v_z\frac{\partial}{\partial z},$$

and

$$D'' = \frac{\partial^2}{\partial r^2} + \frac{1}{r}\frac{\partial}{\partial r} + \frac{1}{r^2}\frac{\partial^2}{\partial\phi^2} + \frac{\partial^2}{\partial z^2}.$$

These equations are supplemented by the no-slip conditions at the end walls ($z = \pm\eta$),

$$v_r = v_\phi = v_z = 0, \text{ at, } z = \pm\eta, \tag{8}$$

and the no-slip conditions at the side wall ($r = 1$),

$$v_r = v_\phi = v_z = 0, \text{ at, } r = 1. \tag{9}$$

The only forcing of the flow quantities comes from the term $-2r\tau_r = 2\varepsilon r\cos\phi$ present in the $z$-momentum equation. When this term vanishes, $\varepsilon = 0$, the governing equations admit the trivial solution $\mathbf{v} \equiv \mathbf{0}$, $p^d \equiv 0$. Hence, the velocity deviation from solid-body rotation is $O(\varepsilon)$. Moreover, if $(v_r, v_\phi, v_z, p^d)$ is the solution at ($r$, $\phi$, $z$), the solution at ($r$, $\phi+\pi$, $-z$) is ($v_r$, $v_\phi$, $-v_z$, $p^d$). These symmetries are exploited to save computational power. Furthermore, in practical applications of interest, the parameter $\varepsilon$ is small, i.e. $\varepsilon \le 0.057$ for $\theta \le 20^o$, $\Omega \le 500$ rpm, and $\omega \ge 3000$ rpm. Since the flow quantities are $O(\varepsilon)$, then for sufficiently small $\varepsilon$, it is well justified (Herbert 1985) to use $\varepsilon$ to linearize the governing equations. When this is done, the continuity equation remains unchanged, while the momentum equations are written in vector form,

$$\frac{\partial}{\partial\phi}\mathbf{v} + 2r\tau_r\mathbf{e}_z + 2\tau\times\mathbf{v} + \nabla p^d - \frac{1}{\mathrm{Re}}\nabla^2\mathbf{v} = 0, \tag{10}$$

where $\mathbf{e}_z$ is a unit vector in the $z$ direction and $\tau = (0, 0, 1+\tau_z)$. These equations support the additional symmetries: $\mathbf{v}(r, \phi+\pi, z) = -\mathbf{v}(r, \phi, z)$ and $p^d(r, \phi+\pi, z) = -p^d(r, \phi, z)$.

## EVALUATION OF MOMENTS

While it is best to use cylindrical coordinates ($r$, $\phi$, $z$) to describe the velocity and pressure, it is convenient to use the aeroballistic reference frame ($x$, $y$, $z$) to express the moment in terms of Cartesian components ($M_x$, $M_y$, $M_z$). It can then be shown (Herbert & Li 1987, 1990;Murphy 1985, 1991) that these components are related to the flow velocities by

$$M_x = 2\frac{\Omega}{\omega}(\rho\omega^2 a^5)\cos\theta\int_{-\eta}^{\eta}\int_0^{2\pi}\int_0^1 v_z r^2\cos\phi\, dr\, d\phi\, dz, \tag{11a}$$

$$M_z = M\tan\theta, \tag{11b}$$

$$M_y = 2\frac{\Omega}{\omega}(\rho\omega^2 a^5)\cos\theta\int_{-\eta}^{\eta}\int_0^{2\pi}\int_0^1 v_z r^2\sin\phi\, dr\, d\phi\, dz$$

$$+\frac{\Omega}{\omega}(\rho\omega^2 a^5)\sin\theta\int_{-\eta}^{\eta}\int_0^{2\pi}\int_0^1 v_\phi r^2\, dr\, d\phi\, dz. \tag{11c}$$

The above formulae are only valid for steady state conditions as it is the case here. For unsteady flows, the reader is referred to the study by Li & Herbert (1991) for appropriate evaluation of the moments.

We represent the velocity field by the Fourier series

$$\mathbf{v}(r,\phi,z) = \sum_{n=-\infty}^{\infty}\mathbf{v}_n(r,z)e^{in\phi},\ \mathbf{v}_n = (u_n, v_n, w_n), \tag{12}$$

where $i^2 = -1$. It is then evident from the expressions of the moments, upon performing the integrations over $\phi$, that we need only consider the Fourier components $w_1$ and $v_0$. If the flow quantities are expanded in powers of $\varepsilon$, it becomes obvious that $w_1$ is $O(\varepsilon)$, since the forcing term in the equations of $O(\varepsilon)$ is simply periodic, and $v_0$ is $O(\varepsilon^2)$. In what follows, we will concentrate on how to solve for $w_1$.

## AXIAL FLOW EQUATIONS

An equation governing $w_1$ has been derived by Selmi, Li, and Herbert (1992). It is based on equations (10) and takes the form

$$\nabla^2 w + \frac{2i}{\mathrm{Re}}\nabla^4 w - \frac{1}{\mathrm{Re}}\nabla^6 w - \tau_\theta^2\frac{\partial^2 w}{\partial z^2} = 0, \tag{13}$$

where $\tau_\theta = 2(1+\tau_z)$, $w_1(r, z)=\varepsilon w(r, z)$, and

$$\nabla^2 = \frac{\partial^2}{\partial r^2} + \frac{1}{r}\frac{\partial}{\partial r} - \frac{1}{r^2} + \frac{\partial^2}{\partial z^2}.$$

The derivation of the boundary conditions that accompany this equation is very tedious and we limit ourselves to just presenting them. Interested readers are encouraged to consult the dissertation by Selmi (1991) for detailed derivations of such boundary conditions. At the end walls ($z=\pm\eta$), these conditions take the form

$$w = 0, \frac{\partial w}{\partial z} = 0, -i\frac{\partial^2 w}{\partial z^3} + \frac{1}{\mathrm{Re}}\left[2\nabla_1^2 \frac{\partial^3 w}{\partial z^3} + \frac{\partial^5 w}{\partial z^5}\right] = 0, \qquad (14)$$

where

$$\nabla_1^2 = \frac{\partial^2}{\partial r^2} + \frac{1}{r}\frac{\partial}{\partial r} - \frac{1}{r^2},$$

while at the side wall ($r=1$), they are

$$w = 0, \qquad (15a)$$

$$-\frac{\partial}{\partial r}(\nabla_1^2 w) - \frac{\partial^3 w}{\partial r \partial z^2} - \tau_\theta \frac{1}{r}\nabla_1^2 w$$
$$-\frac{i}{\mathrm{Re}}\left[\frac{\partial}{\partial r}(\nabla_1^4 w) + 2\frac{\partial}{\partial r}\nabla_1^2 \frac{\partial^2 w}{\partial z^2} + \frac{\partial^5 w}{\partial r \partial z^4}\right] = \tau_\theta \mathrm{Re}, \qquad (15b)$$

$$-\frac{1}{r}\nabla_1^2 w + \tau_\theta i\,\mathrm{Re}\frac{\partial w}{\partial r} - \tau_\theta \frac{\partial}{\partial r}(\nabla_1^2 w)$$
$$-2\tau_\theta \frac{\partial^3 w}{\partial r \partial^2 z^2} - \frac{i}{r}\frac{1}{\mathrm{Re}}\left[\nabla_1^4 w + 2\nabla_1^2 \frac{\partial^2 w}{\partial^2 z^2}\right] = \tau_\theta \mathrm{Re}. \qquad (15c)$$

## CHEBYSHEV EXPANSION

Before presenting the details of the solution of Eq. (13) subject to boundary conditions (14) and (15), we like to mention that when $w$ was expanded in a straight-forward double Chebyshev series in $r$ and $z$ and the governing equations were satisfied by collocation, the convergence of the solution was poor. We suspect this is due to the singularity of the solution at the corners.

To remedy this problem, we find it best to split the solution into two parts, one corresponds to the infinitely long cylinder that is readily expressed

in terms of analytical functions and another solution we seek. The resulting boundary conditions for the newly sought solution are homogeneous at the corners. In addition, an asymptotic analysis near the corners revealed that such a solution behaves smoothly and much simpler than the one of the original formulation. This leads us to believe that we could achieve better convergence when we adopt the new formulation. Since the solution corresponding to the infinitely long cylinder satisfies Eq. (13), the newly sought solution is also governed by this equation. We thus assume a solution to equation (13) of the form

$$w = -i\left[r - \frac{I_1(qr)}{I_1(q)}\right] + \sum_{m=1}^{M+2N+2}\sum_{n=1} c_{mn}\varphi_m(r)\psi_n(z) \tag{16}$$

where $I_1$ is the modified Bessel function of order 1 and $q^2 = i$ Re. In equation (16), the first term on the right hand side is the solution corresponding to the infinitely long cylinder and for the second term, the basis functions $\varphi_m$ and $\psi_n$ are linear combinations of Chebyshev polynomials,

$$\varphi_m(r) = T_{2m+1}(r) - T_{2m-1}(r), \tag{17}$$

$$\psi_n(z) = [(n-1)^2 T_{2n}(z/\eta) - n^2 T_{2n-2}(z/\eta)]/n^2. \tag{18}$$

The above choice of expansion functions permits us to satisfy the no-slip condition at the side walls and the no-gradient condition at the end walls implicitly. Note that we have exploited symmetry by choosing even polynomials in $z$ and odd polynomials in $r$.

We substitute the assumed solution into the governing equations and the rest of the boundary conditions that were not satisfied implicitly---two at one end wall and two at the side wall. The resulting equations are satisfied in the least squares sense at the *Gauss-Radau* collocation points,

$$r_j = \cos\left(\frac{j\pi}{2M+1}\right),\ j = 0,\cdots,M, \tag{19}$$

$$z_k = \eta\cos\left(\frac{k\pi}{2N+1}\right),\ k = 0,\cdots,N, \tag{20}$$

to solve for the Chebyshev coefficients $c_{mn}$.

For this expansion, we have also found that it is critical to satisfy the governing equation at the boundaries. We suspect this is due to the rapid change of the solution and its derivatives near the walls especially at high Reynolds numbers. The complexity of the boundary conditions prevents us from knowing whether a spectral convergence could be achieved. Because we had to satisfy the equation on the boundaries and some of the conditions at the corners become degenerate, we were not able to cluster the collocation points in such a way as to obtain the same number of algebraic equations as the number of unknown coefficients. Therefore, we have chosen the collocation points in such a way as the number of equations exceeds the number of unknowns and have used the discrete least squares approach to solve such a system.

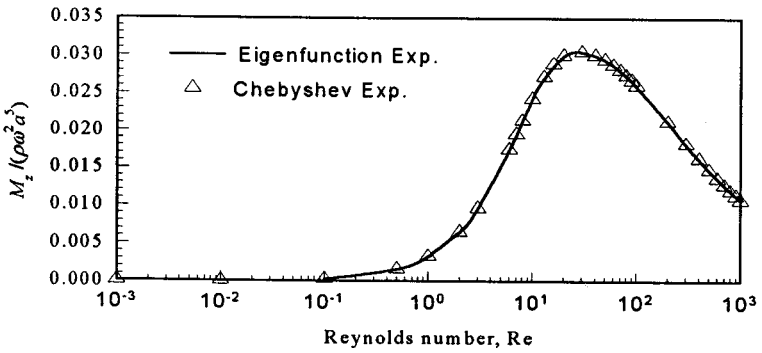


**Figure 2: Dimensionless roll moment versus Reynolds number for $\tau=0.16667$, $\eta=4.368$, and $\theta=20^{o}$. Comparison of the results obtained by eigenfunction expansion (—) and those obtained by Chebyshev expansion (Δ)**

## CALCULATION OF MOMENTS

We use the volume integral approach which has been discussed in a previous section to calculate the moments. We find

$$M_x = 8\pi\eta\tau^2 \cos\theta \sin\theta\,(\rho a^5 \omega^2)\, Real\{\tilde{S}\}, \qquad (21)$$

$$M_y = 8\pi\eta\tau^2 \cos\theta \sin\theta (\rho a^5 \omega^2) Real\{i\widetilde{S}\}, \tag{22}$$

where

$$\widetilde{S} = -i\left[\frac{1}{4} - \frac{I_2(q)}{qI_1(q)}\right] + \sum_{m=1}^{M+2}\sum_{n=1}^{N+2} c_{mn} \int_0^1 r^2 \varphi_m(r) dr \int_0^1 \psi_n(\eta z) dz, \tag{23}$$

and $I_2$ is the modified Bessel function of order 2. Note that the moments can be made dimensionless by scaling them using $(\rho a^5 \omega^2)$.

We have calculated these moments for $\tau = 0.16667$, $\eta = 4.368$, $\theta = 20^\circ$, and a wide range of Reynolds number. The results for the roll, pitch, and yaw moments are shown as functions of Reynolds number in figures 2 through 4 respectively. The results were obtained with a Chebyshev series of 38 × 38 ($N=M=36$) polynomials and the computation for a given value of the Reynolds number takes about 157 seconds on a Cray Y-MP8/864. In the same figures, we plotted the moments obtained by eigenfunction expansion (Selmi et. al, 1992) and as can be seen the results compare very well. For detailed comparisons, we have tabulated these moments obtained by the Chebyshev expansion in table 1 and those obtained by eigenfunction expansion in table 2. A quick glance at both tables reveals that the values agree to within 4 digits of accuracy.

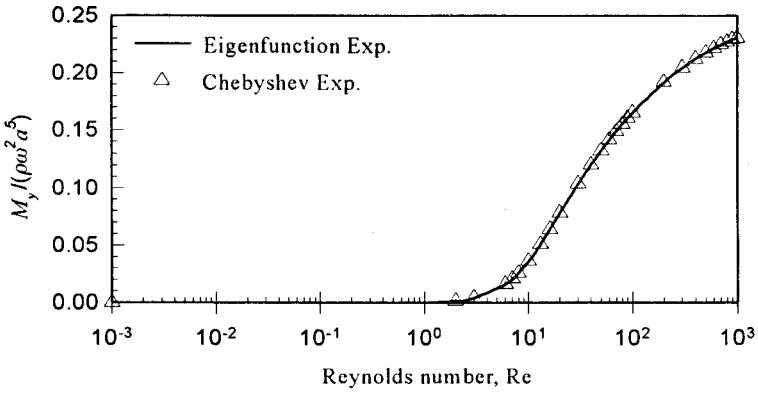


**Figure 3: Dimensionless pitch moment versus Reynolds number for $\tau = 0.16667$, $\eta = 4.368$, and $\theta = 20^\circ$. Comparison of the results obtained by eigenfunction expansion (—) and those obtained by Chebyshev expansion (Δ)**

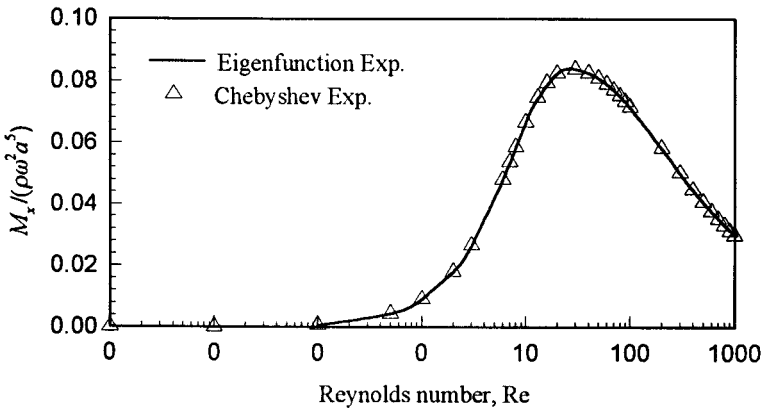


**Figure 4: Dimensionless yaw moment versus Reynolds number for $\tau=0.16667$, $\eta=4.368$, and $\theta=20^{\circ}$. Comparison of the results obtained by eigenfunction expansion (—) and those obtained by Chebyshev expansion (Δ)**

We have also calculated these moments at constant Reynolds number but with different number of polynomials in the expansion. Table 3 and 4 show the values computed for Re=20 and Re=1000 respectively. The results for the error between the moments computed by the Chebyshev expansion and high resolution values obtained by eigenfunction expansion are shown in figures 5 and 6 for Re=20. At this relatively low Reynolds number, the moments converge to within 4 digits of accuracy with at least 20 polynomials in each direction. However, the number of polynomials increases as the Reynolds number increases. For Re=1000, figures 7 and 8 show that the number of polynomials in each direction must be in excess of 35 polynomials in order to achieve similar accuracy.

**Table 1: Dimensionless moments versus Reynolds number obtained by 38×38 Chebyshev expansion for Re=20, $\eta$=4.368, $\tau$=0.16667, and $\theta=20^{o}$**

| $M_x/(\rho\omega^2 a^5)$ | $M_y/(\rho\omega^2 a^5)$ | $M_z/(\rho\omega^2 a^5)$ | Re |
|---|---|---|---|
| .000010 | .000000 | .000004 | .001000 |
| .000748 | -.000283 | .000272 | .100000 |
| .004434 | -.000356 | .001614 | .500000 |
| .009066 | -.000019 | .003300 | 1.000000 |
| .018067 | .001608 | .006576 | 2.000000 |
| .026556 | .004234 | .009666 | 3.000000 |
| .048014 | .016216 | .017476 | 6.000000 |
| .053714 | .021045 | .019550 | 7.000000 |
| .058702 | .026064 | .021366 | 8.000000 |
| .066721 | .036252 | .024284 | 10.000000 |
| .082432 | .078284 | .030003 | 20.000000 |
| .083760 | .103709 | .030486 | 30.000000 |
| .082560 | .120231 | .030049 | 40.000000 |
| .080834 | .132174 | .029421 | 50.000000 |
| .078966 | .141425 | .028741 | 60.000000 |
| .077073 | .148913 | .028052 | 70.000000 |
| .075206 | .155159 | .027373 | 80.000000 |
| .073394 | .160484 | .026713 | 90.000000 |
| .071651 | .165102 | .026079 | 100.000000 |
| .058311 | .191909 | .021224 | 200.000000 |
| .050140 | .204589 | .018249 | 300.000000 |
| .044637 | .212284 | .016246 | 400.000000 |
| .040626 | .217570 | .014787 | 500.000000 |
| .037537 | .221483 | .013662 | 600.000000 |
| .035058 | .224530 | .012760 | 700.000000 |
| .032989 | .226977 | .012007 | 800.000000 |
| .031211 | .228956 | .011360 | 900.000000 |
| .029680 | .230521 | .010803 | 1000.000000 |

**Table 2: Dimensionless moments versus Reynolds number obtained by eigenfunction expansion for Re=20, $\eta$=4.368, $\tau$=0.16667, and $\theta$=20°**

| $M_x/(\rho\omega^2 a^5)$ | $M_y/(\rho\omega^2 a^5)$ | $M_z/(\rho\omega^2 a^5)$ | Re |
|---|---|---|---|
| .000754 | -.000278 | .000275 | .100000 |
| .004470 | -.000316 | .001627 | .500000 |
| .009064 | .000029 | .003299 | 1.000000 |
| .018029 | .001647 | .006562 | 2.000000 |
| .026455 | .004245 | .009629 | 3.000000 |
| .047924 | .016156 | .017443 | 6.000000 |
| .058635 | .025972 | .021341 | 8.000000 |
| .066683 | .036166 | .024271 | 10.000000 |
| .072499 | .046040 | .026387 | 12.000000 |
| .082446 | .078213 | .030008 | 20.000000 |
| .083760 | .103651 | .030486 | 30.000000 |
| .082544 | .120167 | .030044 | 40.000000 |
| .080800 | .132113 | .029409 | 50.000000 |
| .078901 | .141385 | .028718 | 60.000000 |
| .076964 | .148908 | .028013 | 70.000000 |
| .075051 | .155200 | .027316 | 80.000000 |
| .073201 | .160577 | .026643 | 90.000000 |
| .071436 | .165245 | .026001 | 100.000000 |
| .058254 | .191969 | .021203 | 200.000000 |
| .049950 | .204306 | .018180 | 300.000000 |
| .044567 | .212322 | .016221 | 400.000000 |
| .040596 | .217592 | .014776 | 500.000000 |
| .037535 | .221467 | .013662 | 600.000000 |
| .035074 | .224468 | .012766 | 700.000000 |
| .033035 | .226880 | .012024 | 800.000000 |
| .031308 | .228872 | .011395 | 900.000000 |
| .029820 | .230548 | .010854 | 1000.000000 |

**Table 3: Convergence of the moments obtained by Chebyshev expansion for Re=20, $\eta$=4.368, $\tau$=0.16667, and $\theta$=20°**

| $M$ | $N$ | $M_x/(\rho\omega^2 a^5)$ | $M_y/(\rho\omega^2 a^5)$ | $M_z/(\rho\omega^2 a^5)$ |
|---|---|---|---|---|
| 6 | 6 | .083250 | .092973 | .030300 |
| 8 | 8 | .083185 | .090297 | .030277 |
| 10 | 10 | .083521 | .081663 | .030399 |
| 12 | 12 | .083266 | .080443 | .030306 |
| 14 | 14 | .082727 | .078275 | .030110 |
| 16 | 16 | .082753 | .078303 | .030120 |
| 18 | 18 | .082511 | .078204 | .030032 |
| 20 | 20 | .082479 | .078191 | .030020 |
| 22 | 22 | .082456 | .078210 | .030012 |
| 24 | 24 | .082443 | .078200 | .030007 |
| 26 | 26 | .082430 | .078211 | .030002 |
| 28 | 28 | .082421 | .078227 | .029999 |
| 30 | 30 | .082419 | .078249 | .029998 |
| 32 | 32 | .082423 | .078266 | .029999 |
| 34 | 34 | .082427 | .078277 | .030001 |
| 36 | 36 | .082432 | .078284 | .030003 |
| 38 | 38 | .082437 | .078289 | .030004 |
| 40 | 40 | .082441 | .078292 | .030006 |
| 42 | 42 | .082445 | .078293 | .030008 |
| 44 | 44 | .082448 | .078293 | .030009 |
| 46 | 46 | .082451 | .078293 | .030010 |
| 48 | 48 | .082453 | .078292 | .030010 |

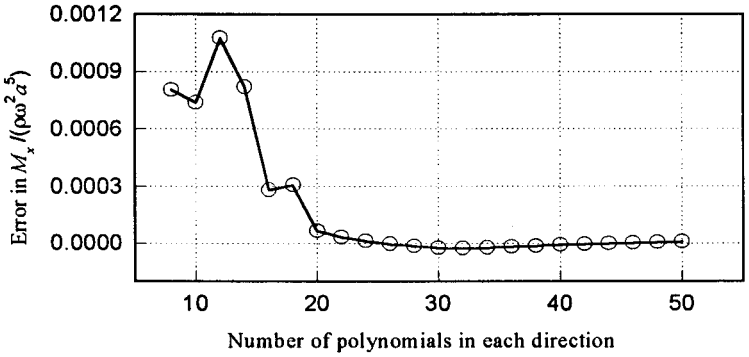


**Figure 5: Error in dimensionless yaw moment versus number of polynomials for Re=20, $\tau$=0.16667, $\eta$=4.368, and $\theta$=20°**

**Table 4: Convergence of the moments obtained by Chebyshev expansion for Re=1000, $\eta$=4.368, $\tau$=0.16667, and $\theta$=20°**

| $M$ | $N$ | $M_x/(\rho\omega^2 a^5)$ | $M_y/(\rho\omega^2 a^5)$ | $M_z/(\rho\omega^2 a^5)$ |
|---|---|---|---|---|
| 6 | 6 | .020448 | .223030 | .007442 |
| 8 | 8 | .020444 | .223027 | .007441 |
| 10 | 10 | .020385 | .222583 | .007420 |
| 12 | 12 | .019625 | .221657 | .007143 |
| 14 | 14 | .019454 | .221570 | .007081 |
| 16 | 16 | .019468 | .221582 | .007086 |
| 18 | 18 | .019518 | .221614 | .007104 |
| 20 | 20 | .019554 | .221639 | .007117 |
| 22 | 22 | .019781 | .221774 | .007200 |
| 24 | 24 | .020157 | .222004 | .007336 |
| 26 | 26 | .020426 | .222218 | .007434 |
| 28 | 28 | .021206 | .222864 | .007718 |
| 30 | 30 | .023099 | .224514 | .008407 |
| 32 | 32 | .027432 | .227860 | .009984 |
| 34 | 34 | .029481 | .229827 | .010730 |
| 36 | 36 | .029680 | .230521 | .010803 |
| 38 | 38 | .029789 | .230708 | .010842 |
| 40 | 40 | .029830 | .230729 | .010857 |
| 42 | 42 | .029836 | .230726 | .010859 |
| 44 | 44 | .029837 | .230723 | .010860 |
| 46 | 46 | .029838 | .230720 | .010860 |
| 48 | 48 | .029838 | .230717 | .010860 |

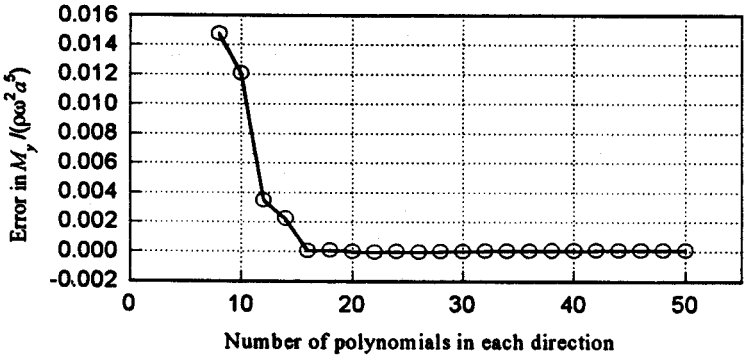


**Figure 6: Error in dimensionless pitch moment versus number of polynomials for Re = 20, $\tau$ = 0.16667, $\eta$ = 4.368, and $\theta$ = 20°**

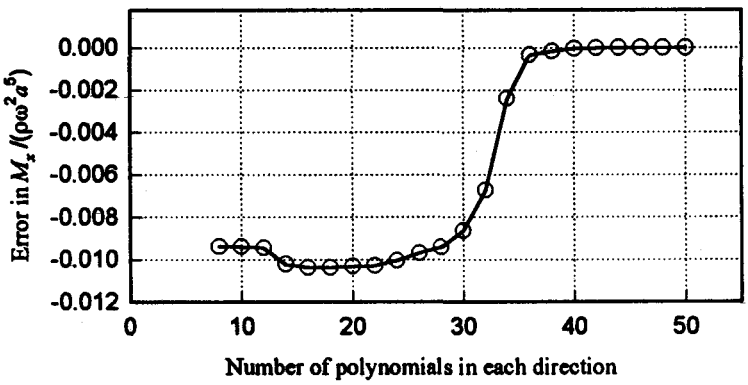


**Figure 7: Error in dimensionless yaw moment versus number of polynomials for Re = 1000, $\tau = 0.16667$, $\eta = 4.368$, and $\theta = 20°$**

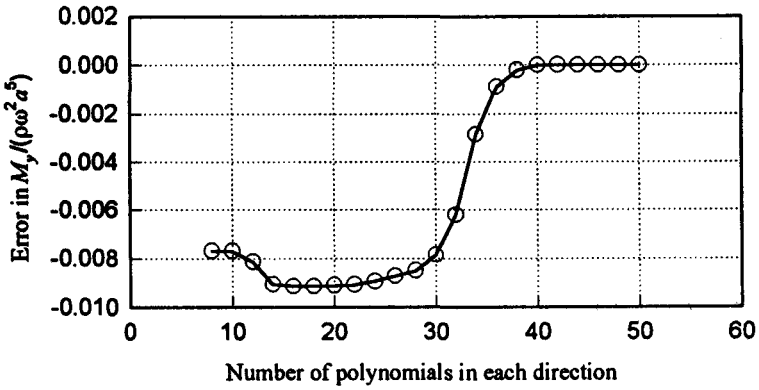


**Figure 8: Error in dimensionless pitch moment versus number of polynomials for Re = 1000, $\tau = 0.16667$, $\eta = 4.368$, and $\theta = 20°$**

We also note from figures 7 and 8 that with relatively low number of polynomials, i.e. 15 to 25 in each direction, the calculated moments do not change significantly with the number of polynomials, yet they do not converge to the values given by eigenfunction expansion. We believe this is

due to the increase in complexity of the solution especially near the corners as the Reynolds number increases, and only a big change in the number of polynomials produces a significant change in the moments. Nevertheless, this method is quite competitive compared to the 3D-spectral code written by Herbert & Li (1987, 1990) since in this approach we are only solving for one Fourier component of one flow quantity in two dimensions and not for a total of 4 quantities in three dimensions. The CPU time and memory allocation are significantly reduced. We also note from the results presented here that certain components of the moments converge faster than others. This has to do with the degree of complexity of the velocity at the plane the moments are heavily dependent on.

## SUMMARY

We have presented an alternative approach to calculating the moments caused by a viscous fluid inside a spinning and coning cylinder. This approach solves the sixth-order partial differential equation describing the axial velocity by spectral collocation. This equation is based on the linearized Navier-Stokes equations and was solved by eigenfunction expansion by Selmi et al. (1992). The eigenfunction approach requires solving a complicated complex eigenvalue problem and accounting for all eigenvalues, which is crucial to the convergence of the method, is a difficult task.

This approach expands the deviation of the axial velocity from that corresponding to an infinitely long cylinder in a triple series in Fourier functions in the azimuthal direction and Chebyshev polynomials in the radial and axial directions. Since only the fundamental component in the azimuthal direction is needed for the evaluation of moments, the expansion is reduced to a double series in Chebyshev polynomials in the radial and axial directions. The expansion coefficients are determined by solving a linear system of equations in the least square sense. The linear system is obtained by satisfying the sixth-order partial differential equation and its boundary conditions at Gauss-Radau points. These points were selected for convenience and Gauss or Gauss-Lobatto points could have been equally utilized.

We have found out that satisfying the governing equation on the boundaries except at the corners speeds up convergence. This in part and the number of boundary conditions that need to be satisfied explicitly prevented us from clustering the collocation points in such a way as to obtain the same

number of equations as the number of unknown expansion coefficients and this leads us to solve the system in the least square sense which has worked quite well. The method is computationally competitive as compared to the 3-D spectral code of Herbert & Li (1987, 1990) and easy to use as compared to the eigenfunction expansion of Selmi et *al.* (1992). Typical runs with 38 × 38 polynomials takes 157 seconds CPU time on a Cray Y-MP8/864.

## ACKNOWLEDGMENTS

We acknowledge the helpful discussions with professor Th. Herbert, Dr. R. Li, and Mr. Miles Miller. All calculations were performed on the Cray Y-MP8/864 of the Ohio Supercomputer Center.

## REFERENCES

**1. Hall, P., Sedney, R. and Gerber, N., 1990.** Dynamics of the fluid in a spinning coning cylinder, AIAA Journal, Vol. 28, No 5, pp. 828-835.

**2. Herbert, Th., 1985.** Viscous fluid motion in a spinning and nutating cylinder. J. Fluid Mech. 167, pp. 181-198.

3. **Herbert, Th. and Li, R., 1987.** A numerical study of the flow in a spinning and nutating cylinder. AIAA Paper No. 87-1445.

**4. Herbert, Th. and Li, R., 1990.** Computational study of the flow in a spinning and nutating cylinder. AIAA Journal Vol 28, No. 9, pp. 1596-1604.

**5. Li, R. and Herbert, Th., 1991.** Numerical study of unsteady 3D Flows in a spinning and nutating cylinder, Proceedings of the 1991 AHPCRC workshop on problems of rotating liquids, University of Minnesota, April 22-23.

**6. Miller, M. C., 1981.** Void characteristics of liquid-filled cylinder undergoing spinning and coning motion, Journal of Spacecraft and Rockets, 18, (3).

**7. Miller, M. C., 1982.** Flight instabilities of spinning projectiles having non-rigid payloads, J. Guidance, Control, and Dynamics, 5, (2).

**8. Murphy, C. H., 1985.** A relation between liquid roll moment and liquid side moment. J. Guidance, Control, Dynamics, 8, pp. 287-288.

**9. Murphy, C. H., 1991.** Moment exerted by a viscous liquid in a spinning, coning, container. Proceedings of the AHPCRC workshop on problems of rotating liquids, University of Minnesota, April 22-23.

**10. Selmi, M., 1991.** Resonance phenomena in viscous fluid configurations inside a spinning and coning cylinder. Ph.D. Dissertation, The Ohio State University, Columbus, Ohio U.S.A.

**11. Selmi, M., Li, R. And Herbert, Th., 1992.** Eigenfunction expansion of the flow in a spinning and nutating cylinder, Physics of Fluids A Vol. 4, No. 9, pp. 1998-2007.

**12. Stewartson, K., 1959.** On the stability of a spinning top containing liquid. J. Fluid Mech. 5,(4), pp. 577-592.

**13. Strikwerda, J. C. and Nagel, Y. M., 1988.** A numerical method for the incompressible Navier-Stokes equations in three-dimensional cylindrical geometry. Journal of Computational Physics, Vol. 78, pp. 64-78.

**14. Vaughn, H. R., Oberkampf, W. L. and Wolfe, W. P., 1985.** Fluid motion inside a spinning nutating cylinder. J. Fluid Mech. 150, pp. 121-138.

**15. Wedemeyer, E. H., 1966.** Viscous corrections to Stewartson's stability criterion. Ballistic Research Laboratory Report 1325.